PHOTOGRAPH THIS SHEET

LEVEL

INVENTORY

DTIC ACCESSION NUMBER

ADA087866

FTD-ID(RS)T-0937-79

DOCUMENT IDENTIFICATION

DISTRIBUTION STATEMENT

ACCESSION FOR

NTIS   GRA&I

DTIC   TAB

UNANNOUNCED

JUSTIFICATION

BY

DISTRIBUTION /

AVAILABILITY CODES

DIST	AVAIL AND/OR SPECIAL	
A		

DISTRIBUTION STAMP

DTIC
SELECTED
AUG 1 5 1980

D
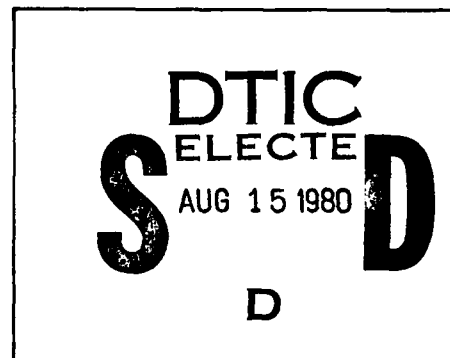
DATE ACCESSIONED

80 6 2 2 81

DATE RECEIVED IN DTIC

PHOTOGRAPH THIS SHEET AND RETURN TO DTIC-DDA-2

DOCUMENT PROCESSING SHEET

FOREIGN TECHNOLOGY DIVISION

COMPARISON OF AERODYNAMIC PROPERTIES OF A CANARD
AIRCRAFT WITH CONVENTIONAL AIRCRAFT

By

Jan Staszek

EDITED TRANSLATION

FTD-ID(RS)T-0937-79   23 October 1979

MICROFICHE NR: FTD-79-C-001381

COMPARISON OF AERODYNAMIC PROPERTIES OF A CANARD
AIRCRAFT WITH CONVENTIONAL AIRCRAFT

By: Jan Staszek

English pages: 24

Source: Prace Instytutu Lotnictwa, Nr. 63, 1975,
         pp. 63-78

Country of Origin: Poland
Translated by: SCITRAN
                F33657-78-D-0619
Requester: FTD/TQTA
Approved for public release; distribution unlimited.

NOMENCLATURE

- b - span
- Cx_s' - drag coefficient of the wing
- Cx_u - canard drag coefficient (elevon drag coef.)
- Cz_s' - wing lift coefficient
- Cz_u - canard lift coefficient (elevon lift coef.)
- Cz_s' - wing lift coefficient in deflected air stream
- Cx_s' - canard lift coefficient in deflected stream (elevon lift coef.)
- C_s - mean chord of wing
- C_u - canard mean chord (mean chord of elevon)
- e - distance behind the trailing edge where horseshoe vortex is fully formed
- K - Kaden's coefficient
- r_r - radius of vortex
- S_s - wing area
- S_u - canard area (elevon area)
- V - velocity
- α - angle of attack
- β - canard (elevon) angle of setting
- ε - angle of air stream deflection
- λ - aspect ratio
- $\sigma = \dfrac{S_u}{S_s}$ - ratio of wing area to area of canard (elevon)

  (* illegible)

1. INTRODUCTION

In the design process of the canard aircraft, it is important to define the influence of the air stream (shed by canard) on the wing. Also a comparison of aerodynamic properties of canard with the conventional aircraft may provide some interesting data.

Because no data was found in the literature on the effect of the aspect ratio, the size of the canard angle of setting and the vertical location of the wing on the aerodynamic properties of the system, polar calculations were made, dependent on changes in the above-stated parameters. In these

calculations, approximate methods were employed and some wind tunnel tests were utilized.

2. DEFLECTION OF AIR STREAM BEHIND CANARD

Due to distortion of the air stream caused by canards, the angle of air stream deflection varies spanwise. It is extremely difficult to mathematically define the speed of the air stream behind the canard because the vortex sheet and tip (horseshoe) vortices are not fully formed yet. The distance behind the trailing edge, where they could be considered formed, was established by Kaden [1]:

$$e = K \frac{\lambda^2}{Cz} c \qquad\qquad (1)$$

For elliptical lift distribution, K = 0.28.

From the above, assuming $\lambda_u = 5$, the distance is

$$e = 7 \frac{c_u}{Cz_u}$$

Considering that the wing is located at a distance equal to $4C_u$ from the canard, it may be assumed that vortices are fully formed when:

$$4c_u = 7 \frac{c_u}{Cz_u} \quad \text{when} \quad Cz_u \cong 1.75$$

This means that for $Cz_u < 1.75$ the flow aft of the canard, where the wing is located, is still in the developmental phase, and the velocity distribution and associated distribution of downwash angles are difficult to define theoretically.

Taking the above into account, the calculations used an experimentally determined distribution of vertical components of air stream velocities aft of the canard; this distribution defined the angles of stream deflection

within the boundaries of the canard span b_u [2]. On the outer part of the wing (beyond the span of the canard) a hyperbolic distribution of velocities according to the equation

$$vr = const$$

was assumed on the basis of velocities experimentally determined for the inner part of the vortex core.

Figure 1 shows the assumed distance between the canard and wing. Figure 4 shows the vertical distance of the wing aerodynamic axis from the aerodynamic axis of the canard.
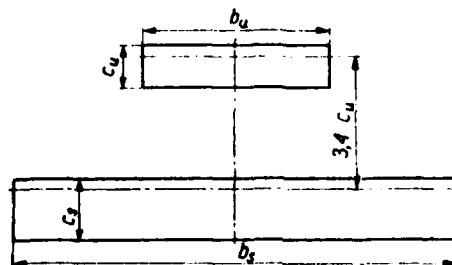

Figure 1. Basic dimensions of the system

$$\lambda_s = 7, \ \lambda_u = 5, \ \sigma = \frac{S_u}{S_s} = 0.3$$

In reality, the canard is usually located at greater distances forward of the wing than shown on Figure 1. We have no experimental data pertaining to the vertical components of the air speed behind the canard, except for those contained in NACA Report 651 [2]. The report gives data for deflection distance equal to 1.3 C_u and 3.4 C_u. The flow in this region is still not formed, and it is difficult to define theoretically. Therefore, for purposes of further discussion, a vertical distance of 3.4 C_u was selected for air speed behind the canard, in accordance with the above-mentioned NACA wind tunnel tests, although in actuality this value will be different for different angles of attack and distances. The difference should not be great, however, although this assertion is not supported by experimental data.

A second simplification is the disregard of the effect of the wing on the deflection of the air stream in front of it. Because of the action of the wing, the angle of attack of the canard is somewhat larger, depending on wing Cz. And in this case the difference was small and was disregarded.

Figure 2 shows the formation and location of the horseshoe vortex in accordance with NACA [2] measurements. Figure 3 shows the angle of air stream deflection along the line where the vertical plane containing the aerodynamic axis of the wing intersects with the horizontal planes, whose vertical distance from the canard aerodynamic axis   is given in units of canard span b_u [2].
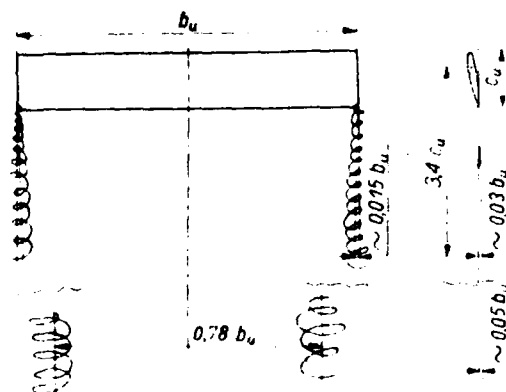
Figure 2.   Location of wing tip vortices at a distance of 3.40 behind the trailing edge and at a much larger distance.
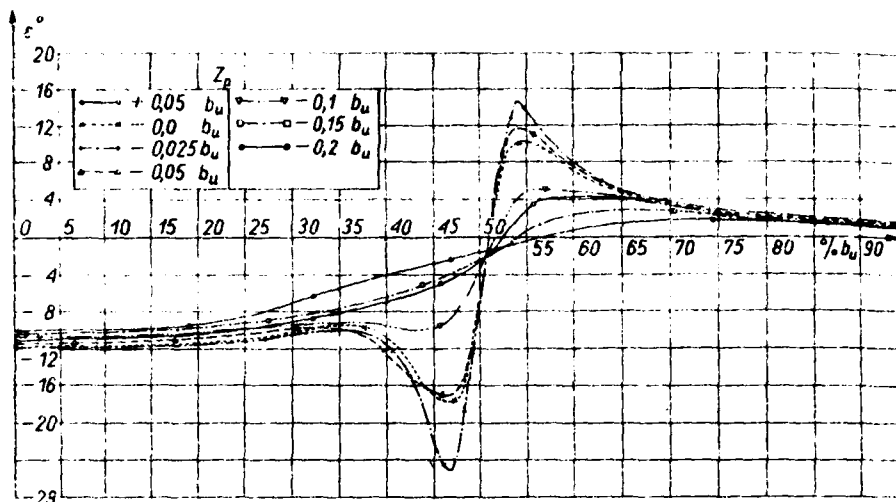
Figure 3.   Angle of air stream deflection along the span of the wing,
when distance between the wing and canard is equal to 3.40_u.

where: $C_z=1.35$, b_u - canard span, λ_u - aspect ratio of canard, Z_p -
vertical distance between aerodynamic axis of wing and the
horizontal reference plane.

Figure 4 shows the geometric construction which provided a definition of

vertical components of flow velocity given by the Rankin vortex, whose axis

and core diameter were also assumed from NACA measurements.   Vortex axis

location is shown on Figures 2 and 3; its core radius at this point is about

3.4% b_u, and its axis is at a distance of about 3% b_u below the horizontal

plane of the aerodynamic axis of the wing.   The axis of the horseshoe vortex

is almost parallel to the direction of undisturbed air flow and does not

shift in the vertical direction as much as it moves aft.   In the horizontal

plane, both vortex branches converge to asymptotes 0.78 b_u apart, at a large

enough distance aft of the canard.

At the distance of concern to us, at the point of the main wing, the

shift of the vortex axis from the end of the wing span to the center does not

exceed 1.5% b_u (vortices axes separating distance is about 0.97 b_u).
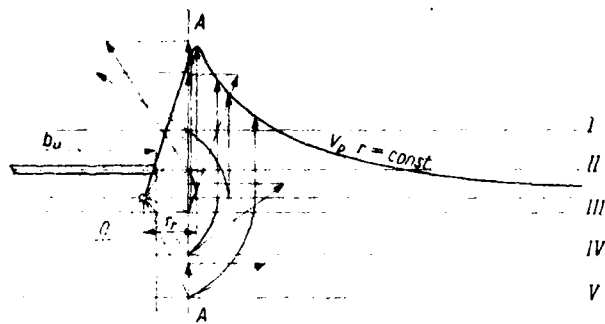
/67

Figure 4. Distribution of vertical components of velocity on
outside of canard wing span;

A-A - plane in which vertical components V were measured,
r_r - vortex core radius, I - distance 0.05 b_u above canard axis,
II - horizontal aerodynamic canard axis, III - distance 0.05 b_u
below canard axis, IV - distance 0.1 b_u below canard axis, V -
distance 0.15 b_u below canard axis, 0 - axis of free vortex.

The angle of air stream deflection in the plane of symmetry is defined
by the equation $/3/$

$$\varepsilon = -\frac{46,2}{\lambda_u} Cz_u \qquad (2)$$

and changes only slightly in the 0.7 b_u range.

Because of this deflection of air streams aft of the canard, the entire
section of the wing located between the axes of the horseshoe vortex flowing
from the canard has the reduced increment ΔCzs ,

since the actual angle of attack α_n is

$$\alpha_n = \alpha - \varepsilon \qquad (3)$$

while its increment is

$$\Delta\alpha_n = \Delta\alpha - \Delta\varepsilon \qquad (3a)$$

Equation 2 indicates that when the aspect ratio is reduced, a situation is obtained which is very disadvantageous for the part of the wing in the zone of interaction of streams aft of the stabilizer between the horseshoe vortex axes, such as in the case where the increase in the angle of attack by $\Delta\alpha$ simultaneously causes an increase in the downwash angle by $\Delta\varepsilon$, balancing reciprocally. This means that the section of the wing located between the axes of the horseshoe vortex formed by the canard does not sustain an increase in angle of attack in relation to the air streams shedding off the canard. In other words, $\frac{\partial Cz_1}{\partial x}$ for this section of the wing is then zero or almost zero. This is the case when $\lambda_u \cong 2.5$ and $\lambda_s \cong 6$. When λ_u is further reduced, the derived $\frac{\partial Cz_1}{\partial x}$ assumes negative values.

Outside the axis of the horseshoe vortex, the situation is just the opposite and increment $\frac{\Delta Cz_1}{\Delta x}$ is larger than for a non-canard wing, for the real angle of attack is

$$\alpha_n = \alpha + \varepsilon \qquad (4)$$

and its increment is

$$\alpha_n = \Delta x + \Delta\varepsilon \qquad (4a)$$

In this case, the angle of air stream deflection varies along the wing span in accordance with the distribution of velocity coming from the free

vortex, as opposed to the previous case, where the angle remained almost uncnanged in the middle region of the horseshoe vortex.

An increase in value of $\frac{\Delta Czs}{\Delta x}$, for this part of the wing is larger <u>outside the vortex axis</u> only in a certain range of angles of attack α, namely until the actual angle of attack α_n assumes a value for which C_{zs} reaches a maximum. If this value is exceeded by α_n, $\frac{\Delta Czs}{\Delta x}$ will assume negative values. On the other hand, $\frac{\Delta Czs}{\Delta \alpha}$ will be positive for the middle section of the wing.

/68 This means that the canard accelerates the separation of streams at the tips of the main wing.

It is evident from the above that the main wing of the canard airplane located in the stream which was disturbed by placing the canard forward, has lower values of Czs_{max} than conventional wings in non-deflected flow.

The situation is somewhat different for the coefficient of drag Cx_s of a wing in a canard system. Figure 5a illustrates forces acting on this portion of the wing which is located between the axes of the horseshoe vortices formed by the forward canard.
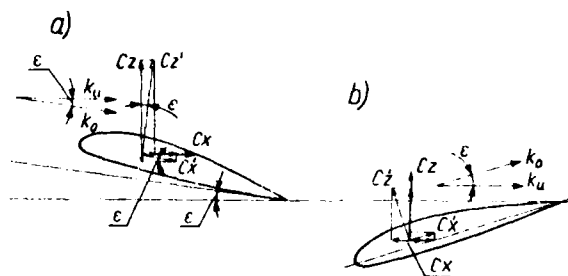
Figure 5. Coefficients of Cz and Cx for canard system wing elements in the direction of undisturbed flow; a) between horseshoe vortices; b) outside; k_u - direction of undisturbed flow; k_o - direction of deflected flow.

This system indicates that in the range of normal flight angles of attack, the coefficient of lift Cz_s of the wing element will always be smaller than in the case of flow-off not disturbed by streams shedding off the canard. However, the drag coefficient Cx_s of this element will always

be larger than in the case of undisturbed flow-off. For undisturbed flow, these coefficients are expressed as follows:

$$Cz = Cz' \cos \varepsilon - Cx' \sin \quad\quad\quad (5)$$

$$Cx = Cx' \cos \varepsilon + Cz' \sin \quad\quad\quad (5a)$$

Of course, as the angle of attack and angle of air stream deflection ε increase, the drag coefficient for the middle element of the wing Cx_s, will increase more rapidly for a canard system wing than the Cx_s drag coefficient for a conventional system wing, where this element is surrounded by the undisturbed stream.

Figure 5b shows the distribution of forces created forward of the canard acting on the element of the wing which is outside the axis of the horseshoe vortex. Due to the fact that the angle of air stream deflection ε here is positive, a larger value of the Cz, lift coefficient is obtained than in the case of an undisturbed airflow.

This increase is caused by adding the sum of Cz' and Cx' projections in the perpendicular direction to the direction of undisturbed flow. In determining the Cx_s drag coefficient, projections of Cx' and Cz' in parallel direction to direction of undisturbed flow are subtracted. Thus:

$$Cz = Cz' \cos \varepsilon + Cz' \sin \quad\quad\quad (6)$$

$$Cx = Cx' \cos \varepsilon - Cz' \sin \quad\quad\quad (6a)$$

Due to such a distribution of aerodynamic forces action on the wing /69 element located outside the axis of the horseshoe vortex, in the range of small angles of attack α, the Cx drag coefficient of this element in the direction parallel to the undisturbed airflow, may be smaller in canard systems than in conventional systems, and in certain cases it may even assume negative values.

3. NONTWISTED WING PROPERTIES OF THE CANARD AIRPLANE

In order to analytically define the influence of air stream deflection aft of the canard on the wing characteristics, the lift coefficient Cz_s and drag coefficient Cx_s of nontwisted wing were calculated, taking stream deflection into account in accordance with the graph shown in Figure 3. The canard system followed that shown in Fig. 1, assuming aerofoil wing section I.A. 608, with aspect ratio $\lambda_s = 7$, and the same section for the canard with aspect ratio $\lambda_u = 5$. Ratio of area of canard to the area of the wing is 0.3, and the assumption was made that the wing is located in a plane 0.075 b_u below the canard plane. Angle of incidence of canard β is equal to 2.5°.

A simplified graph of the distribution of angles of air stream deflection along the wing span is shown in Fig. 6. Values of the angles of deflection in the plane of symmetry were calculated from equation (2). Values of angles of air stream deflection ϵ for various wing elements were taken from Figure 3, using angles of deflection in the plane of symmetry as a reference.
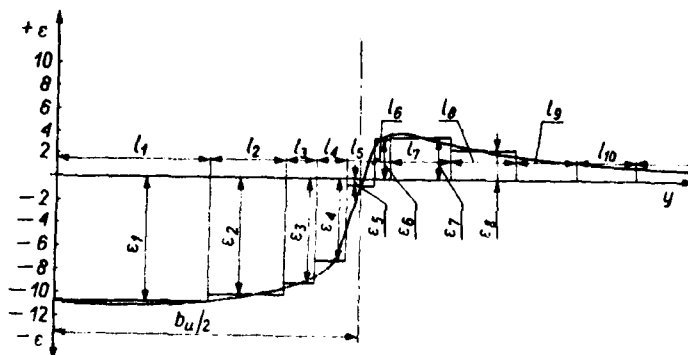
Figure 6. Simplified graph of air stream deflection along the wing span, at a distance of 3.4 c_u behind the aerodynamic axis of canard, and 0.075 b_u below.

where:

a_1	a_2	a_3	a_4	a_5	a_6	a_7	a_8	a_9	a_{10}
.5	.25	.1	.1	.1	.05	.2	.2	.2	.2

$a_n - 2l_n/b_u, \, \epsilon_n - \epsilon_1 w_p, \, \epsilon_n$ - angle of stream deflection at a given point (from Figure 3),

w_p - coefficient dependent on relocating the wing and changing the angle of attack (obtained from Figure 3).

Coefficients C_z and C_x for the specific wing elements were calculated from equations (5), (5a), (6), (6a) and true angles of attack for these elements were determined from equations (3), (3a), (4), (4a).

Results are shown in the form of the polar curve for an untwisted wing in Figure 8. For comparison the same figure shows the polar curve of the same wing in airflow stream not disturbed by deflections from forward canard.

From the above comparison, it is evident that the influence of the deflected stream is very great, particularly at large angles of attack where

/70 we observe an increase in drag coefficient C_x and a decrease in the coefficient of lift C_z with a distinctly large flattening of the polar curve. At small angles of attack, however, drag coefficient C_x is smaller than for a wing in flow undeflected by canard. Because of this fact, in addition to other basic considerations for using the canard system, placing the

canard ahead of the main wing may be advantageous in high-speed planes, hence at small angles of attack. This phenomenon is explained by the existence of a well-placed large coefficient of lift C_z' for wing elements located outside the horseshoe vortex. This coefficient (C_z') reduces the local drag coefficient C_x', as shown by equation (6a).

The obtained result is not encouraging because the anticipated increase in lift coefficient C_z of the entire system is reduced by the negative effect of the deflection of air streams shed from the canard onto the main wing. This makes it necessary to seek corrective measures to at least partially eliminate the undesirable effects of the forward canard on the main wing.

The greatest stream deflection aft of the canard occurs close to the axis of the horseshoe vortex, as can be seen in Fig. 3. If the wing is located further than $1.8\ r_r$ under or over the vortex axis, then the entire range of high gradients of angles of stream deflection ϵ is beyond the wing and the aerodynamic properties of the canard are correspondingly worse. It can thus be concluded that the II and III wing positions shown on Fig. 4 and Fig. 7, are not advantageous, because in flight at functional angles of attack the core of the vortex shedding from the canard strikes the main wing. As a result, the negative effects and angles of stream deflected, discussed above, are largest.

Figure 7. Position of the vortex for different angles of attack in a canard system.
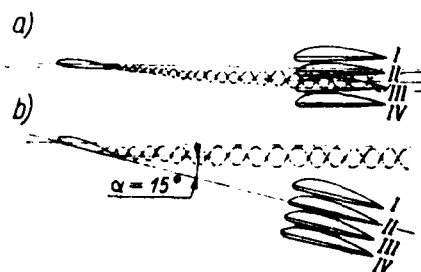
Because the axis of the horseshoe vortex is constant in relation to the direction of undisturbed flow, wing location I, over the vortex core (Fig. 7) is only seemingly good, because when the airplane angle of attack is increased, the vortex core strikes the main wing, causing an undesirable increase in

stream deflection. It is true that at an angle of attack on the order of $\alpha = 15°$ the vortex core is beyond the main wing, but at intermediate angles the wing is under the direct effect of the vortex core.

Locating the wing in position IV is most advantageous, because the vortex core is always beyond the wing, and moves away from it as angles of attack become larger. Taking into account the above circumstances, all canard system calculations were made on the assumption that the wing will be in position IV, it being the most justified. At the same time this determines the canard design will be a low-wing monoplane with a forward canard located as high as possible.

4. CANARD TWISTED WING PROPERTIES

The most effective way to improve geometric properties of the wing is by twisting it geometrically so that the true angles of attack of airfoil elements in deflected airflow will give a favorable distribution of lift along the wing span (close to elliptical). It is thus necessary to calculate the angle of air stream deflection ε behind the canard for each wing element and then place each element at an angle corresponding to the angle of stream deflection. Because the angle of stream deflection ε, as is shown by equation (2), is proportional to the canard lift coefficient (Cz_u), the wing twist must correspond to only one angle of attack. This preferred angle of attack α_0 should be defined in the initial aerodynamic analysis of the airplane, taking into account its design and prevailing flight conditions.

To analytically determine the effect of airfoil twisting, coefficients of lift and drag for a wing of the canard system shown on Fig. 1 were calculated. The wing was twisted according to the plan shown in Fig. 6. Profiles and airfoil surfaces of the canard system were assumed the same as in the case of an untwisted wing and at the same angle of canard setting $\beta = 2.5°$.

Twisting was calculated for the preferred angle of attack of the wing $\alpha_\bullet = 2.5^\circ$, for which $Cz = 0.7$. A polar curve was obtained by applying equations (5) and (5a), (6) and (6a) for each airfoil element and then summing up the results for the specific angles of attack.

As a result, a canard system twisted wing polar curve was obtained which showed the coefficient Cx_{min} to be 40% larger and the Cz_{max} coefficient to be 6% larger than for an untwisted wing. A comparison of both polar curves is made in Fig. 8.

By decreasing preferred angle α_0, Cx_{min} becomes smaller, but at the same time Cz_{max} also decreases, bringing the shapes of the polar curves close to that of the shape for the untwisted curve. The nature of the changes is shown in Fig. 9.
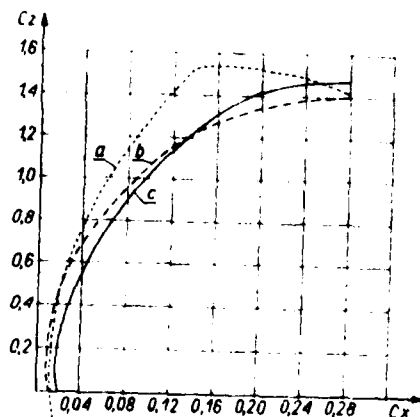
Figure 8. Comparison of polar curves for wing in undisturbed airflow   with canard wings for $\sigma = 0.3$, $\beta = 2.5^\circ$
$\lambda_\bullet = 5$, $\lambda_1 = 7$

a) - conventional design; b) - canard with nontwisted wing;
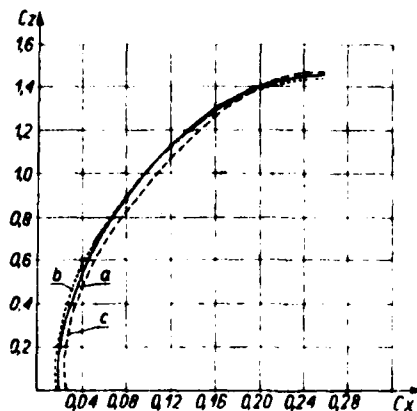c) - canard with twisted wing for $\alpha_0 = 2.5^\circ$.

Figure 9. Correlation between preferred angle α_0, angle of setting, and the polar curve . a) – reference wing $\alpha_0 = 2.5^o$, $\beta_0 = 2.5^o$, $\sigma = 0.3$, $\lambda_u = 5$; b) – twisted wing, $\alpha_0 = 0^o$, $\beta_0 = 2.5^o$, $\sigma = 0.3$, $\lambda_u = 5$; c) – twisted wing, $\beta = 5^o$, $\alpha_0 = 2.5^o$, $\sigma = 0.3$, $\lambda_u = 5$.

An increase in angle of canard setting β also increases the angle of stream deflection ϵ, and, in doing so, increases the effect of stream deflection Cz_{max}. Cz_{min} then also become smaller. The changes are shown in Fig. 9.

As could be predicted, a decrease in canard area lessens its effect on the wing, and its polar curve is distinctly improved, as shown in Fig. 10.

Moving the wing downward from the vortex core has a positive effect because deformation of the airflow and size of angles of stream deflection are smaller. As an example, a recalculation was made of the polar curve of the wing located at $x = 0$ in the axis of the free vortex and the polar curve moved down $0.05\ b_u$. Results are shown on Fig. 10.
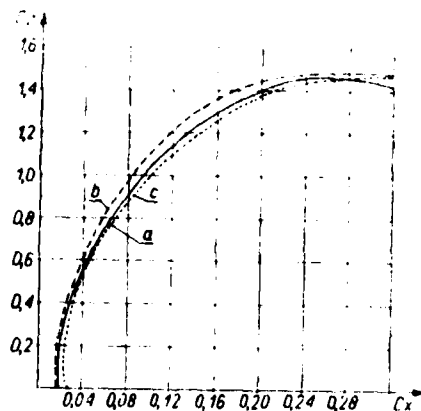
Fig. 10. Influence of canard size and wing
location on shape of polar curve.

a - reference wing, $\sigma = 0.3$, $\alpha_0 = 2.5^o$, $\beta = 2.5$
$\lambda_* = 5$ located 0.05 b_u below vortex axis

b - wing with smaller canard, $\sigma = 0.2$ and
$\alpha_0 = 2.5^o$, $\beta = 2.5$, $\lambda_* = 5$ located
0.05 b_u below vortex axis

c - wing located at $x = 0$ in vortex axis;
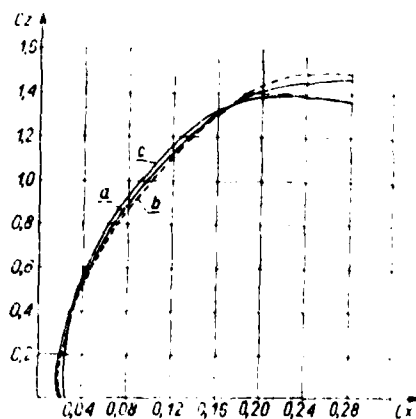$\alpha_0 = 2.5^o$, $\beta = 2.5^o$, $\sigma = 0.3$, $\lambda_* = 5$

Figure 11. Canard aspect ratio vs. polar curve
shape, where:
$\alpha_0 = 2.5^o$, $\beta = 2.5^o$, $\sigma = 0.3$, $\lambda_* = 5$
a - reference wing, $\lambda_* = 5$;

b - wing with aspect ratio, $\lambda_* = 7$

c - wing with aspect ratio, $\lambda_* = 3$

Increase in the canard aspect ratio λ_u from 5 to 7 caused no

significant changes in the shapes of the polar curves with the exception of

a small increase in Cz_{max}, which is shown in Fig. 11. An analysis of this

has determined than an increase in canard aspect ratio lessened the effect

of the outside portion of the horseshoe vortex and, despite the smaller

angle of stream deflection, the unfavorable influence of deflection remained

almost unchanged. The beneficial effect of increasing the aspect ratio

appears only when the wing span (or aspect ratio) of the wing is increased

at the same time to maintain the same proportions of wing encompassed by

negative and positive angles of stream deflection ε . To confirm this thesis,

a polar curve is shown calculated for canard aspect ratio $\lambda_u = 3$. In

actuality, a better shape was obtained in the middle portion of the curve,

/73 but this was at the cost of decreased Cz_{max} and increased Cx_{min}. In this

aspect the tandem arrangement of canard and wing spans of equal length is

least advantageous (in view of lower increment ΔC_z of wing in comparison

with canard, which makes it impossible to obtain Cz_{max} for both surfaces

simultaneously. It should be added that canard coefficient $\frac{\partial Cz}{\partial x}$ grows with

an increase of aspect ratio, which is undesirable from the standpoint of

directional stability.

The effect of changes in canard aspect ratio on wing polar curve of the

same span and aspect ratio is shown in Fig. 11.

5. COMPARISON OF TWISTED WING CANARD SYSTEM WITH CONVENTIONAL SYSTEM

Because the canard is very important in producing lift, a comparison of

the wings alone in the canard system and the usual system is not conclusive.

For this reason polar calculations were made for both compared systems,

taking into account canards with deflected elevons. As the comparative

conventional system, the same untwisted wing was assumed and a canard with a JA177 airfoil and aspect ratio $\lambda_k = 3.35$.

Because in the conventional system it is necessary to apply downward force due to the deflection of the elevons and the need to obtain Cz_{max}, a force equal to 4% of the wing lift was assumed [1]. For the canard system, the same value of upward force, 4% of wing lift, was assumed, and added to the canard in view of elevon deflection necessary to obtain Cz_{max}.

In comparing both polar curves shown in Fig. 12, it is seen that in the case of the canard, the lift coefficient Cz_{max} of the entire system is about 40% higher than for the conventional system. However, Cx_{min} increases 80%. The canard system, then, is best when the decisive indicator in the airplane construction concept is the highest lift coefficient Cz_{max}.

The comparison of curves $Cz/Cx = f(\gamma)$ on Fig. 13, permits further comparison of both systems. The maximum Cz/Cx ratio in the conventional system is always greater than in canard system. It is true that after adding parasitic drag of the magnitude $Cx_{szk} = 0.03$, the differences are distinctly smaller, however the conventional system is still better from the standpoint of lift/drag ratio in the entire range of angles of attack. Thus from the standpoint of flight properties and airplane glide angle, the conventional system is superior.

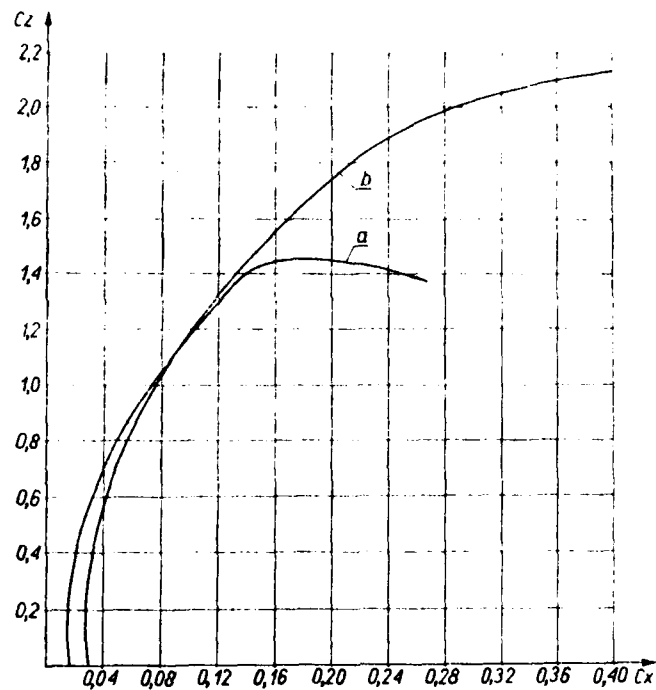[1] This is the average amount obtained for several airplanes.

Figure 12. Comparison of polar curves of conventional and
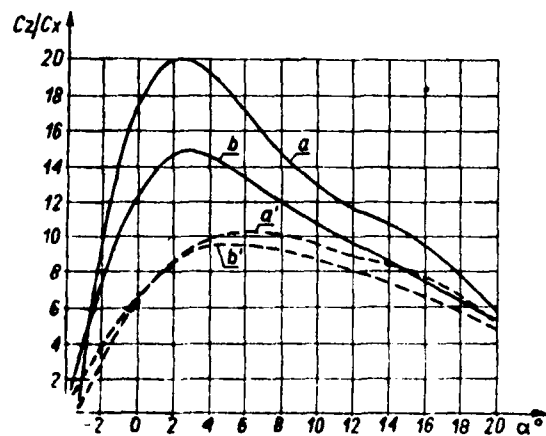canard airplanes
a) conventional design; b) canard

Figure 13. Comparison of $Cz/Cx = f(\alpha)$ for canard and conventional
aircraft
a, a′ = conventional system; b, b' - canard;a', b' -
canard (including parasitic drag)

Another typical system indicator, so-called $Cz^3/Cx^2 = f(Cz)$ is also more advantageous to the conventional system if only the wing and canard are compared. However, the curve describing the canard is flatter and the large value of Cz^3/Cx^2 coefficient covers a longer range than in the conventional system (Fig. 14). The situation changes when parasitic drag factors are added, because the $(Cz^3/Cx^2)_{max}$ ratio for the canard system applies at larger angles of attack and at larger values of Cz coefficient. With the right amount of parasitic drag, the canard system can be more advantageous than the conventional system, although with small parasitic drag the usually applied wing-canard configuration is undoubtedly better.

In the case examined, with parasitic drag $Cx_{szk} = 0.03$, the value of $(Cz^3/Cx^2)_{max}$ was somewhat smaller for the conventional system than for the canard system.
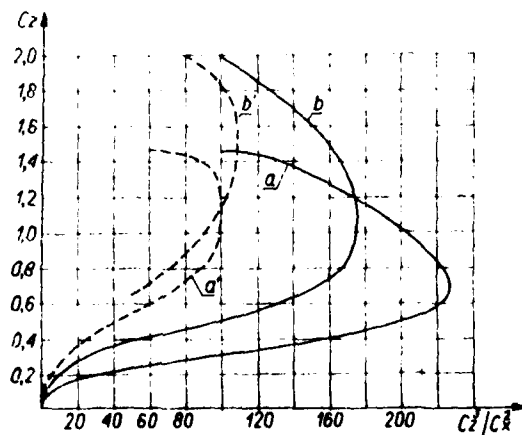
/75

Figure 14. Comparison of $\frac{Cz^3}{Cx^2} = f(Cz)$ for the canard and conventional design.

a-a' - conventional design; b-b' canard design; a'b' - canard when parasitic drag was taken into account

6. CENTER OF PRESSURE TRAVEL

To define the center of pressure travel in the canard system, the position of aerodynamic force resultant as a function of the angle of attack was calculated for the same system. This is necessary to determine the effect of canard system on allowable shift in center of gravity.

Calculations were made on the assumption that aerodynamic forces of the wing and canard are located in the aerodynamic axis of every lift area (wing and canard) at a distance of 25% of the chord length measured from the leading edge of the airfoil. Thus the calculations did not include the center of pressure travel for each surface separately during change in angle of attack, but take into account only the shift in aerodynamic force resultant from the assumed canard system.

It should be noted that the influence of air stream deflection on shift of aerodynamic force resultant is negative from the standpoint of directional stability. Although $-\frac{\partial C_z}{\partial x}$ is smaller for the canard because of its lower aspect ratio, the stream deflection in the region between axes of the horseshoe vortex decreases $\frac{\partial C_z}{\partial x}$ for this part of the wing so effectively, that in this case the mean coefficient $\frac{\partial C_z}{\partial x}$ is lower for the entire wing than for the canard, even though the sections of the wing outside the vortex have a higher $\frac{\partial C_z}{\partial x}$ than the wing in undisturbed flow. This phenomenon was discussed in greater detail in Section 2.

/76 As shown by the curves in Fig. 15, the shift in center of pressure is dependent also on the deflection angle β. The distance of travel is significant and for change of 0 to 5° in angle of attack (change of C_z from 0.413 to 0.937) is equal to 6% of wing chord length for $\beta = 2.5^{\circ}$.
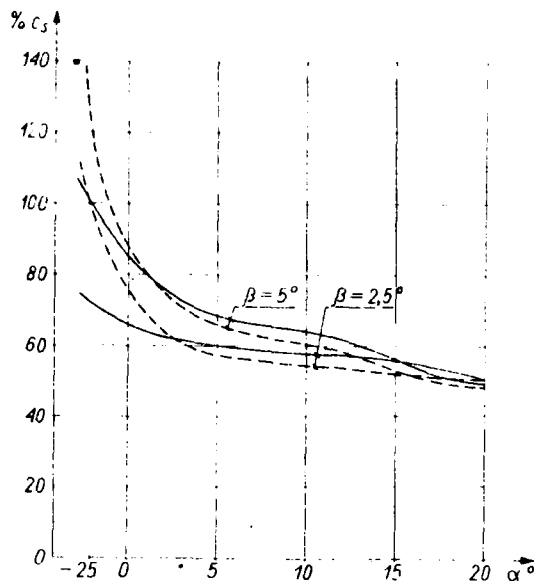
Figure 15. Canard center of pressure vs. angle of incidence.

$\sigma - 0.3$, $\alpha_o = 2.5^o$, $\lambda_u = 5$, $\lambda_s = 7$.

- distance given in percent of wing chord in forward direction from aerodynamic axis of wing

- distance of wing axis from canard axis is $3.4\ c_u$

- dashed line shows course of change in positions of pressure centers in the case of canard stream deflection.

When deflection angle $\beta = 5^o$, the distance of pressure travel for α from 0° to 5° (value of C^{ι} changes from 0.508 to 0.997) is 17.5% of the wing chord.

Corresponding values in a case of undisturbed flow would be-- $\beta = 2.5^o$, a travel distance of 18% of wing chord, at change in angle of attack from 0° to 5°. But for $\beta = 5^o$ travel distance of pressure center would be 23% of wing chord.

These values were calculated for a $3.4\ c_u$ (canard chord) distance between aerodynamic axes of the wing and canard. These values rise as distances between aerodynamic axes of canard and wing increase.

7. CONCLUSION

In summing up the obtained results and the present knowledge of the canard, the following conclusions may be drawn.

1. By using a forward horizontal wing in the canard type plane, the total lift of the canard-wing system is increased by a value approximate to the ratio of the flight control surfaces to the area of the wing. Thus, it is possible to reduce the weight of the plane by making better use of the canard, thereby increasing the payload. This has a decisive effect on the economy of using high-frequency flights for short distances.

2. The ratio $\frac{Cz}{Cx}$ for a canard sytem is worse than for a conventional system, except in the case of an untwisted wing at relatively small angles of attack. In this case, however, we have a much lower value of lift coefficient Cz_{max}. The canard system is not suitable for long range planes where economy or small angle of glide is a deciding factor. From this standpoint canard construction is inferior to conventional design.

3. The ratio $(Cz^3/Cx^2)_{max}$ for the wing-canard assembly itself is worse in the case of the canard system; however, if the entire airplane is considered, the opposite may be true. For planes in which it is not possible to obtain high values of aerodynamics because of their design, the relatively large values of parasitic drag favor the canard and a larger ratio $(Cz^3/Cx^2)_{max}$ can be obtained than for the conventional system. The result is that the speed of ascent and minimum thrust required for take-off are better with the canard design in the case where the entire airplane cannot be aerodynamically clean. This is important in ordinary transport or agricultural planes or those of similar purpose.

4. Because of the small drag coefficient Cx_{min} of the untwisted wing at small angles of attack, the canard system may be advantageous for high-speed

planes which are equipped with the proper wing mechanization to obtain large values of lift coefficient Cz_{max}. Considering also the permissibly large travel of the aerodynamic center of pressure in the near-sonic speed range, the canard system is a good design for high-speed aircraft.

5. Placing canards in front of wings helps during landings and take-offs because of the ground effect. In the case of the canard, the ground effect helps in attaining larger lift on the horizontal canard. In the conventional system, this effect is negative, because in order to reach a larger angle of attack and attain Cz_{max}, the elevon must be deflected more to obtain sufficient downward force.

6. The material presented shows where to seek optimum solutions for a plane system with a forward flight surface. Not all of the problems have been thoroughly investigated and those of longitudinal and lateral stability have been omitted entirely. This must be treated separately.

Submitted February, 1975

BIBLIOGRAPHY

1. *Spreiter J. R. and Sacks A.*: Trailing vortex sheet effect on downwash. J.A.S. January 1951.
2. *Silverstein A., Katzow A. and Bullivant W. A.*: Downwash and wake behind plain and flapped airfoils, NACA, Rep. 651, 1939.
3. *Ostoslawski J. W.*: Aerodynamika samolcta, Oborongiz, Moskwa. 1957.
4. *Gates S. B.*: Notes on the tail-first aeroplane. R.M. 2676, July 1939.

Comparison of Some Aerodynamic Properties of a Canard and a Conventional Airplane

Summary

An attempt is made to represent in a quantitative manner the advantages and the drawbacks of a Canard Airplane to be taken into consideration during the early design work. The range of the lift and drag coefficient of the wing alone and the wing with the control surfaces are determined for the canard airplane and compared with those for the conventional system. The action of the air stream leaving the elevator and flowing towards the main wing is discussed as well as methods for reducing the influence of downwash by means of:
   application of a twisted wing to achieve the required angle of incidence
   correct selection of control surface setting
   correct selection of aspect ratio for the control surfaces
   correct location of the wing with respect to the control surfaces.
As a result of the analysis it is found that the canard system has, under some conditions, properties approaching those of the conventional system and that it is, for some configurations, more advantageous as regards the possibility of obtaining maximum lift.

DISTRIBUTION LIST

DISTRIBUTION DIRECT TO RECIPIENT

ORGANIZATION		MICROFICHE	ORGANIZATION		MICROFICHE
A205	DMATC	1	E053	AF/INAKA	1
A210	DMAAC	2	E017	AF/RDXTR-W	1
B344	DIA/RDS-3C	9	E403	AFSC/INA	1
C043	USAMIIA	1	E404	AEDC	1
C509	BALLISTIC RES LABS	1	E408	AFWL	1
C510	AIR MOBILITY R&D LAB/FIO	1	E410	ADTC	1
C513	PICATINNY ARSENAL	1		FTD	
C535	AVIATION SYS COMD	1		CCN	1
C591	FSTC	5		ASD/FTD/NIIS	3
C619	MIA REDSTONE	1		NIA/PHS	1
D008	NISC	1		NIIS	2
H300	USAICE (USAREUR)	1			
P005	DOE	1			
P050	CIA/CRB/ADD/SD	2			
NAVORDSTA (50L)		1			
NASA/NST-44		1			
AFIT/LD		1			
LLL/Code L-389		1			
NSA/1213/TDL		2			

FTD-ID(RS)T-0937-79